DOI: https://doi.org/10.24425/amm.2026.1981

PAWEŁ PRUSKO[1*], DOROTA MOSZCZYŃSKA[1], RAFAŁ MOLAK[1], JAROSŁAW MIZERA[1]

ANALYSIS OF MECHANICAL PROPERTIES OF IN 718 PRODUCED BY COLD METAL TRANSFER

Wire Arc Additive Manufacturing (WAAM) has emerged as a promising technology for the fabrication of large-scale metallic components due to its high deposition rate and efficient material utilization. Among various WAAM approaches, the Cold Metal Transfer (CMT) process is characterized by reduced heat input, stable arc behavior, and low spatter generation, making it particularly suitable for processing nickel-based superalloys. In this study, Inconel 718 components were fabricated using the WAAM-CMT technique and systematically compared with conventionally manufactured reference material. The investigation focused on the relationship between processing conditions, microstructural evolution, defect formation, and resulting mechanical properties in the as-deposited state as well as after post-processing, including Hot Isostatic Pressing (HIP) and subsequent heat treatment. The results indicate that WAAM-CMT processing leads to reduced mechanical performance in the as-built condition ($R_m \approx$ 550-720 MPa). However, the application of HIP combined with optimized heat treatment significantly improves the mechanical properties through defect elimination, microstructural homogenization, and precipitation strengthening ($R_m \approx$ 1100-1250 MPa). As a result, the mechanical performance of the processed material approaches or even exceeds that of the reference material.

Keywords: Inconel; Cold Metal Transfer; Heat treatment; Mechanical properties; Microstructure

1. Introduction

Inconel 718 is a precipitation-hardened nickel-based superalloy widely used in aerospace, energy, and offshore applications due to its exceptional combination of high-temperature strength, corrosion resistance, weldability, and resistance to creep, fatigue, and stress-rupture degradation [1-3] Its superior mechanical performance is primarily derived from precipitation strengthening by metastable γ'' (Ni_3Nb) and γ' ($Ni_3(Al,Ti)$) phases, which are formed during aging and provide the main strengthening contribution in service conditions up to approximately 650-700°C [4]. In chloride-containing environments, the alloy benefits from its Cr-rich matrix, which promotes passive film formation, while the combined presence of Ni and Mo enhances resistance to pitting, crevice corrosion, and stress corrosion cracking. These characteristics make Inconel 718 particularly suitable for turbine components, heat exchangers, fasteners, and subsea production systems operating under combined thermal, mechanical, and corrosive loading [5,6].

Subsea production trees, often referred to as "Christmas trees" [7-9], represent one of the most demanding application areas for Inconel 718. These systems are installed on subsea wells to regulate production, injection, and shut-in functions through a network of valves, chokes, and sensors. During service, they are exposed to high hydrostatic pressure, low ambient temperature, corrosive seawater, and chemically aggressive internal media containing CO_2, H_2S, or hydrogen-rich fluids. Because intervention costs are extremely high and accessibility is limited, subsea trees must provide outstanding structural integrity, corrosion resistance, and long-term reliability over extended service lifetimes.

Although Inconel 718 is traditionally manufactured by casting or forging followed by extensive thermomechanical processing and heat treatment, these routes are associated with high material waste, long lead times, and limited design freedom. These limitations have stimulated growing interest in additive manufacturing as a route for producing complex nickel-based components more efficiently. Among the available metal additive manufacturing techniques, Wire Arc Additive Manufacturing (WAAM) is especially attractive for large-scale structures because of its high deposition rate, high material utilization, and relatively low feedstock cost [10,11]. In particular, Cold Metal Transfer (CMT) is of interest due to its controlled droplet transfer, low heat input, reduced spatter, and lower tendency for distortion and defect formation [12].

[1] WARSAW UNIVERSITY OF TECHNOLOGY, FACULTY OF MATERIALS SCIENCE AND ENGINEERING, 141 WOŁOSKA STR., 02-507 WARSAW, POLAND

* Corresponding author: pawel.prusko.dokt@pw.edu.pl

Seow et al. [13] showed that WAAM-produced Inconel 718 is highly sensitive to post-deposition heat treatment, with the as-built condition exhibiting microsegregation, Laves phase formation, and strong anisotropy associated with columnar solidification. Importantly, they demonstrated that optimized heat-treatment schedules can dissolve detrimental Laves phase, improve microstructural homogeneity, and partially restore tensile properties, although the final performance remained below that of wrought material. In agreement with these findings, subsequent studies on CMT-WAAM Inconel 718 confirmed that the as-deposited state is typically characterized by coarse columnar grains, dendritic segregation, and limited mechanical performance, whereas tailored post-processing promotes precipitation of strengthening phases and substantial improvement in strength and ductility. In another study, Li et al. [14] investigated the influence of shielding gas composition on WAAM-fabricated Inconel 718 and showed that it strongly affects arc stability, bead geometry, and defect formation. A 2% H_2 + Ar mixture provided the most favorable process stability and defect reduction, highlighting the importance of shielding gas optimization in WAAM.

Despite these advantages, WAAM-fabricated Inconel 718 often still exhibits anisotropic properties and inferior performance in the as-built condition. For this reason, post-processing routes such as hot isostatic pressing (HIP) and heat treatment are critical for mitigating porosity, reducing segregation, promoting precipitation of strengthening phases, and improving the overall mechanical response.

Accordingly, the present study attempts to address the existing knowledge gap concerning the possibility of achieving the desired properties of IN718 alloy manufactured by the WAAM-CMT process in combination with post-processing treatments, with particular emphasis on the role of HIP and heat treatment in reducing process-induced heterogeneity and restoring properties closer to those of conventionally processed material.

This study aims to investigate the mechanical properties and microstructural characteristics of IN718 fabricated via additive manufacturing, with a focus on its suitability for application in components of underwater petrochemical installations.

2. Experimental

The studied material was a nickel-iron superalloy, Inconel 718, obtained from a conventionally manufactured bar with a diameter of 70 mm. The material was in the forged and heat-treated condition, consistent with standard industrial practices applied in the production of subsea components. The microstructure of the bar in the initial condition was revealed using optical microscopy. Equiaxed grains were observed, characteristic of a material subjected to thermomechanical processing and subsequent heat treatment. The average grain size, determined using stereological methods, was 69,2 µm, 80,4 µm, 74,6 µm – Fig. 1. In each analyzed case, the microstructure was examined using optical microscopy (Keyence VHX-7000). The observations were conducted in three orthogonal directions in order to obtain a comprehensive description of grain size and morphology, as well as to identify any potential material discontinuities, such as cracks and porosity Vickers microhardness measurements (HV0.2, applied load 0.49 N, dwell time 10 s) were carried out along the principal build orientations (XY, XZ, YZ) in accordance with ASTM E384. For each measurement location, a minimum of ten indentations was performed to ensure statistical reliability. Uniaxial tensile tests were conducted at room temperature on miniaturized specimens using a universal testing machine (Zwick/Roell Z005 equipped with a 5 kN load cell) at a constant crosshead speed of 0,005 mm·sec^{-1}. The mechanical response was evaluated in terms of yield strength ($R_{0.2}$), ultimate tensile strength (R_m), uniform elongation, and fracture strain. Three specimens were tested for each material variant and orientation to ensure statistical reliability of the results. Standard deviations were calculated.

Microstructural observations were performed using a Hitachi SU70 scanning electron microscope (SEM). SEM/EDS analysis of the distribution of alloying elements, including area mapping and point analysis, were also performed. Prior to examination, the specimens were prepared using a standard metallographic procedure to ensure a high-quality surface suitable for microstructural characterization. The samples were sequentially ground using SiC abrasive papers, followed by polishing with diamond

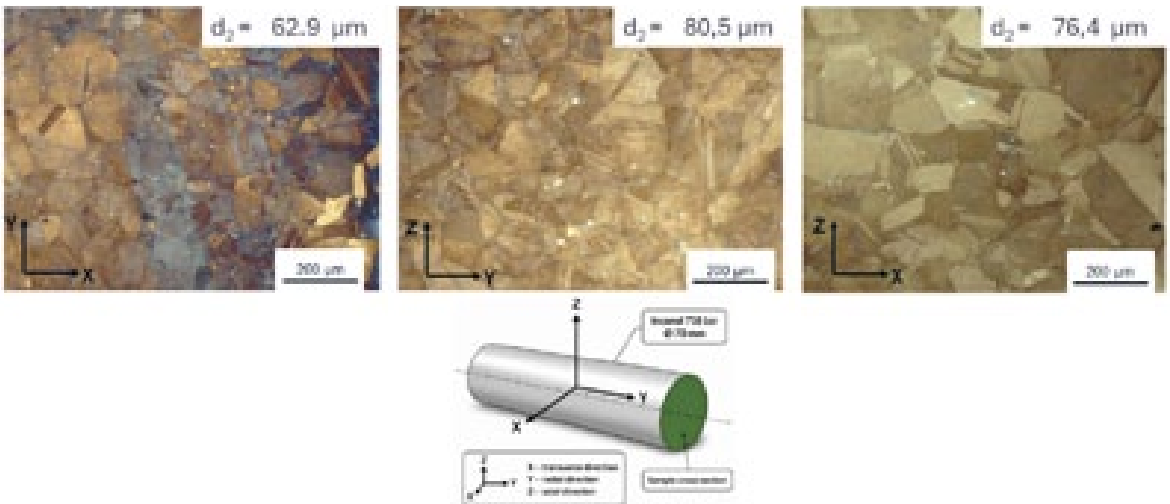

Fig. 1. Microstructure of Inconel 718 in the initial state

suspensions of progressively decreasing particle size. To further improve the surface quality and minimize preparation-induced deformation, vibratory polishing was applied as a final mechanical polishing step. Subsequently, the specimens were subjected to low-energy Ar^{+} ion milling using an Ion Milling System (Hitachi IM4000) to remove the residual mechanically affected surface layer and obtain a deformation-free surface for SEM analysis.

Additive manufacturing was carried out using a wire arc additive manufacturing (WAAM) system based on cold metal transfer (CMT) technology – Fig. 2. The setup consisted of a six-axis ABB IRB 6200 robotic arm integrated with a Fronius TPS 500i CMT power source. A 1.2 mm diameter Inconel 718 wire (TABLE 1) was used as feedstock and deposited under a purified argon shielding atmosphere. The torch-to-substrate distance was kept constant at 8 mm to ensure stable arc conditions and repeatable melt pool geometry. The current used was between 240 A and 200 A, adjusted across wall height of deposited material. The torch travel speed was 6.5 mm/s, and the wire feed speed was adjusted between 1.5 and 2 m/min. Depending on the applied parameters, the layer height varied between 2.0 and 2.5 mm, resulting in differences in local heat input and thermal cycling conditions. Three parameter sets were employed to investigate the influence of process conditions on thermal history, microstructural evolution, and mechanical properties: (i) WAAM CMT 350 INC718, optimized for weld stability and material quality; (ii) WAAM CMT 150 AC INC718, aimed at achieving a high deposition rate through enhanced material transfer; and (iii) WAAM CMT 150 INC718, optimized for reduced energy input and process cost. In the following sections, these conditions are referred to as CMT 350, CMT 150AC, and CMT 150, respectively. The applied parameter sets led to different solidification conditions, cooling rates, and interlayer reheating effects, thereby affecting grain morphology, segregation behavior, and defect formation. For each parameter set, wall-type specimens

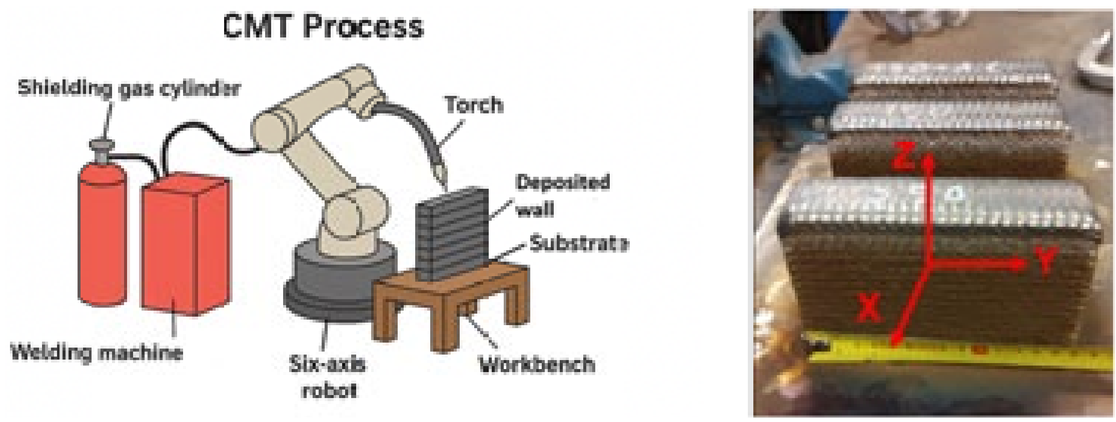

Fig. 2. CMT process setup and deposited walls

TABLE 1

Chemical composition of 3D print Alloy IN718 wire (wt.%)

C	Si	Mn	P	S	Cr	Mo	Ni	Cu	Ti	Al	Nb	B	Fe
0,05	0,06	0,11	0,004	0,001	17,54	3,01	52,46	0,02	0,88	0,47	5,15	0,002	20,05

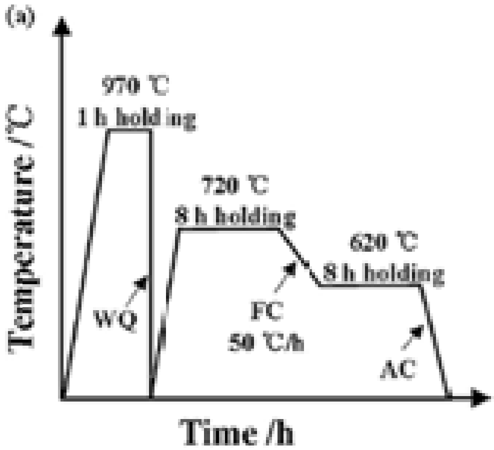

Fig. 3. Heat treatment cycle of Inconel 718 showing solution treatment, water quenching (WQ), and two-stage aging with controlled furnace cooling (FC) and final air cooling (AC)

with nominal dimensions of approximately 40×70×150 mm were fabricated. This geometry ensured the development of quasi-steady thermal conditions along the build height, enabling correlation between processing parameters, microstructural features, and mechanical properties.

The CMT deposited walls were subjected to two stage post-processing that involved hot isostatic pressing (HIP) and heat treatment (HT). The hot isostatic pressing (HIP) procedure was carried out under the following conditions: 1200°C, 2 h, 200 MPa, and argon atmosphere. Subsequently, a two-step heat treatment was applied, consisting of solution treatment at ~970°C for 1 h followed by water quenching, and a two-stage aging process involving aging at ~720°C for 8 h with furnace cooling to ~620°C, followed by second aging at ~620°C for 8 h and final air cooling. The scheme of post-process heat treatment condition is depicted in Fig. 3.

3. Results

3.1. As-Built WAAM-CMT Condition

The microstructure of Inconel 718 alloy observed by optical microscopy in the as-built condition following WAAM-CMT processing is characterized by strong anisotropy resulting from the layered nature of solidification. It consists of dendritic columnar grains oriented parallel to the deposition direction. Microscopic observations revealed distinct interlayer bands and reheating zones arising from repeated thermal cycles during the deposition process – Figs. 4a), b); 5a), b) and 6a), b).

In the longitudinal section, grains were elongated and continuous across multiple layers, whereas the transverse section revealed a mosaic arrangement of dendritic colonies. The observed morphology is characteristic of directional solidification under high thermal gradients and corresponds to the typical "cast-like" microstructure of WAAM materials – Figs. 4a) b); 5a), b) and 6a), b). Scanning electron microscopy (SEM) observations revealed, for each applied processing variant, distinct areas of individual columnar grains and a well-developed network of dendritic cell boundaries – Figs. 7a), b); 8a), b); 9a), b). A typical structure formed during rapid directional solidification in the WAAM process is visible: a γ-matrix with segregation of Nb and Mo into interdendritic regions, where Laves phase (Ni,Fe,Cr)\$_2$(Nb, Mo, Ti) forms (bright, irregular precipitates). Branched γ/ Laves eutectic precipitates were also identified in the CMT350 condition – Fig. 9a), b).

The presence of carbide and nitride precipitates (NbC, TiN) was also revealed – very small bright particles visible in SEM images – Figs. 7b); 8b); 9b). Phase identification for each manufacturing variant and post-processing condition was performed based on precipitate morphology analysis and EDS chemical composition analysis (an example is shown for CM350 – Fig. 9c)-g).

The mechanical properties of the investigated Inconel 718 alloy produced by WAAM-CMT depend both on the additive

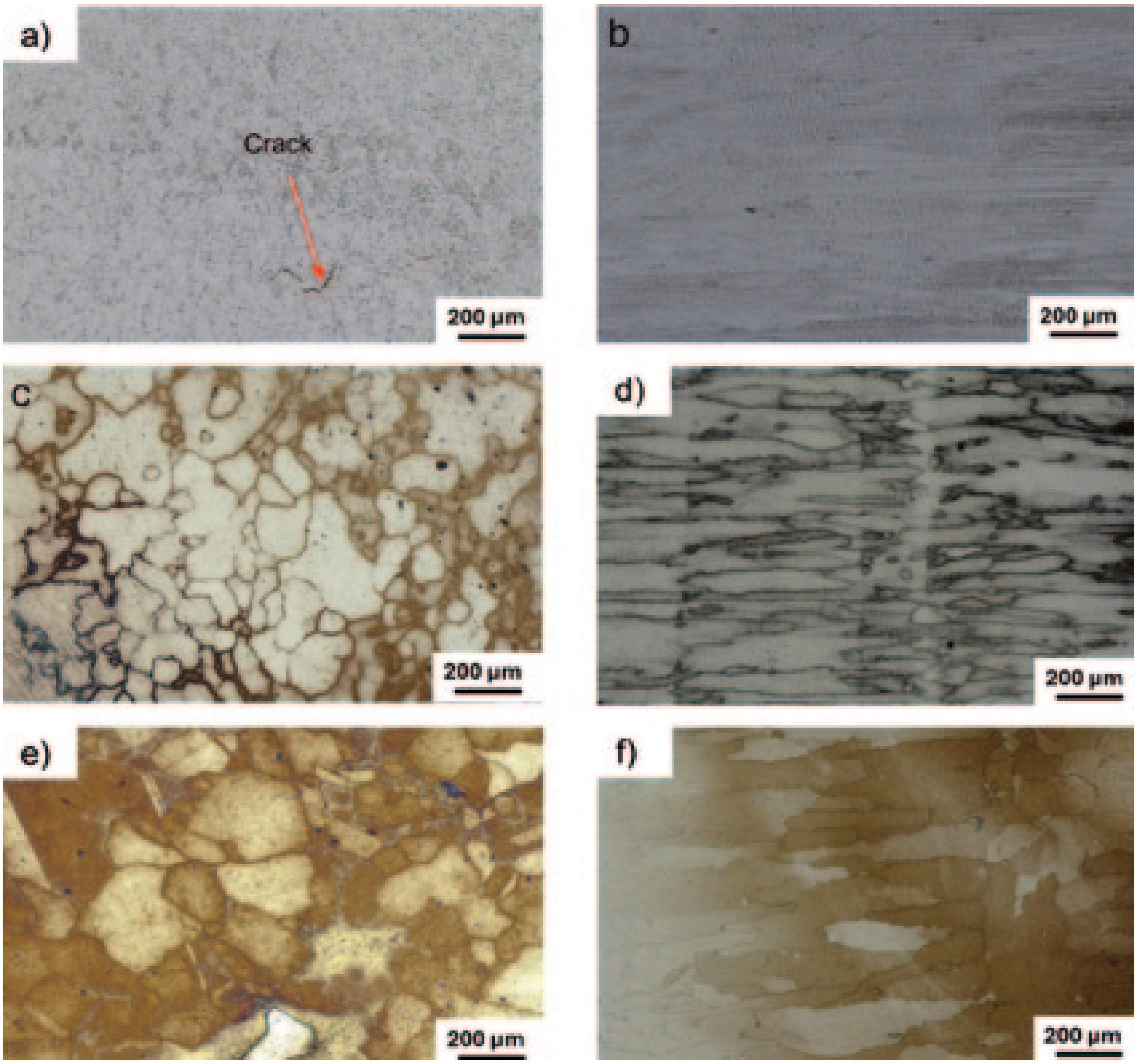

Fig. 4. Cross-section OM images of CMT 150 material variants in two perpendicular planes (a), c), e) – XY plane and b), d), f) – YZ plane): a), b) as deposited; c), d) after HIP process; e), f) after HIP and HT

manufacturing process parameters and on the applied post-processing treatments.

In the as-built condition, the material exhibited relatively low hardness in the range of 250-270 HV0.2, as well as relatively low yield strength ($R_{2.0}$ ≈ 380-420 MPa) and tensile strength (R_m ≈ 550-720 MPa). These values were significantly lower than those of the reference material (420 HV0.2, $R_{2.0}$ ≈ 850 MPa and R_m ≈ 1140 MPa – Figs. 13-14). This can be attributed to the presence of discontinuities such as pores and microcracks (e.g. Figs. 4a); 5b); 6b)), the dendritic microstructure formed during solidification, and the presence of Laves phase in interdendritic regions – Figs. 7b); 8b) and 9b).

3.2. Effect of post-processing treatment

Following Hot Isostatic Pressing (HIP) conducted at 1200°C for 2 h under a pressure of 200 MPa, the microstructure of Inconel 718 produced by WAAM-CMT exhibited a significantly densified and homogenized microstructure resulting from pore closure, diffusion-driven homogenization, and the dissolution of segregation-induced phases. The combined effect of high pressure and elevated temperature promoted the closure of internal porosity and the diffusion-assisted elimination of microvoids. Simultaneously, interdendritic segregation was reduced and the Laves phase network present in the as-built condition was largely dissolved. The original columnar-dendritic morphology became less distinct due to grain boundary migration and grain growth at the HIP temperature. As a result, the HIP-treated condition exhibited a more homogeneous microstructure – Figs. 4c), d); 5c), d) and 6c), d).

These observations are confirmed by electron microscopy studies. SEM analysis revealed well-defined grain boundaries resulting from recrystallization and grain growth. The dendritic structure typical of WAAM virtually disappeared – Figs. 7c), d); 8c), d); 10a), b).

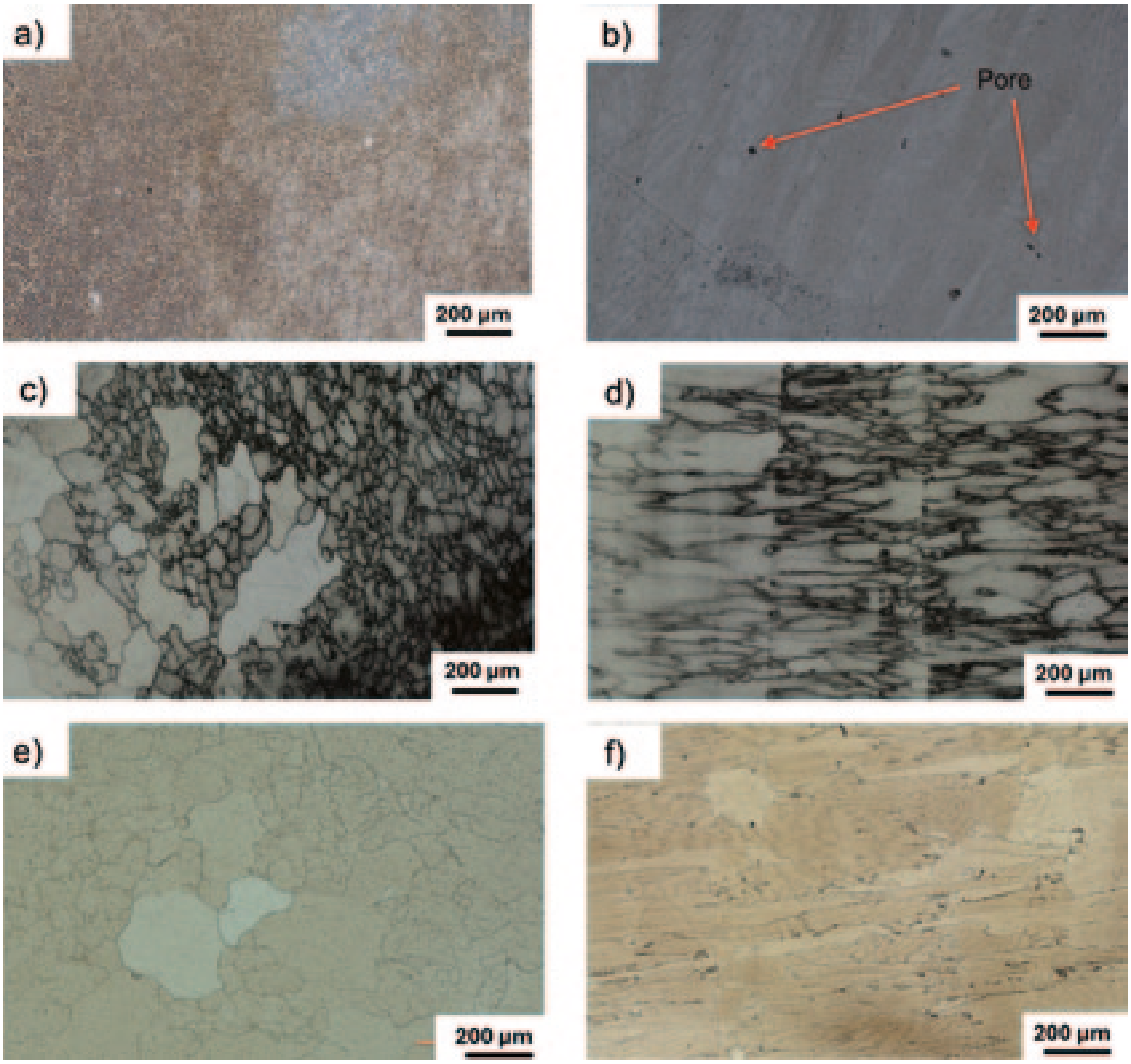

Fig. 5. Cross-section OM images of CMT 150AC material variants in two perpendicular planes (a), c), e) – XY plane and b), d), f) – YZ plane): a), b) as deposited; c), d) after HIP process; e), f) after HIP and HT

Compared to the as-built condition, the continuous bright interdendritic network was no longer observed. This indicates that the Laves phase largely dissolved during HIP at 1200°C, since this temperature is well above the dissolution temperature of both the γ/Laves eutectic and the Laves phase, leading to their nearly complete disappearance. Numerous bright particles distributed within the grains and along grain boundaries were also observed (carbides and nitrides NbC/TiN) – Figs. 7d); 8d); 10b).

After applying post-HIP heat treatment (solution treatment at approximately 970°C for 1 h, water quenching, followed by two-step aging at 720°C and 620°C), the microstructure of Inconel 718 transformed from a defect-containing solidification structure into a dense precipitation-strengthened state. The HIP process eliminated most porosity and reduced interdendritic microsegregation, while solution treatment further dissolved residual Laves phase and homogenized the matrix – Figs. 4e), f); 5e), f) and 6e), f).

SEM observations confirmed the complete disappearance of the dendritic microstructure characteristic of the as-built WAAM condition, as well as the elimination of interlayer bands. The resulting microstructure consisted of recrystallized γ grains with sizes ranging from several tens to several hundreds of micrometers. Neither the dendritic morphology nor the Laves phase and γ/Laves eutectic constituents were observed after HIP treatment. Instead, MC-type carbides and nitrides, mainly NbC and TiN, were identified predominantly along grain boundaries – Figs. 7e), f); 8e), f); 11a), b); 12.

A substantial improvement in mechanical properties was observed following HIP processing. The hardness increased to approximately 320-340 HV0.2 (an increase of about 25%), while the yield strength and ultimate tensile strength reached approximately 430-600 MPa and 700-840 MPa, respectively, depending on specimen orientation (Fig. 13-14). This improvement can be attributed primarily to the elimination of internal

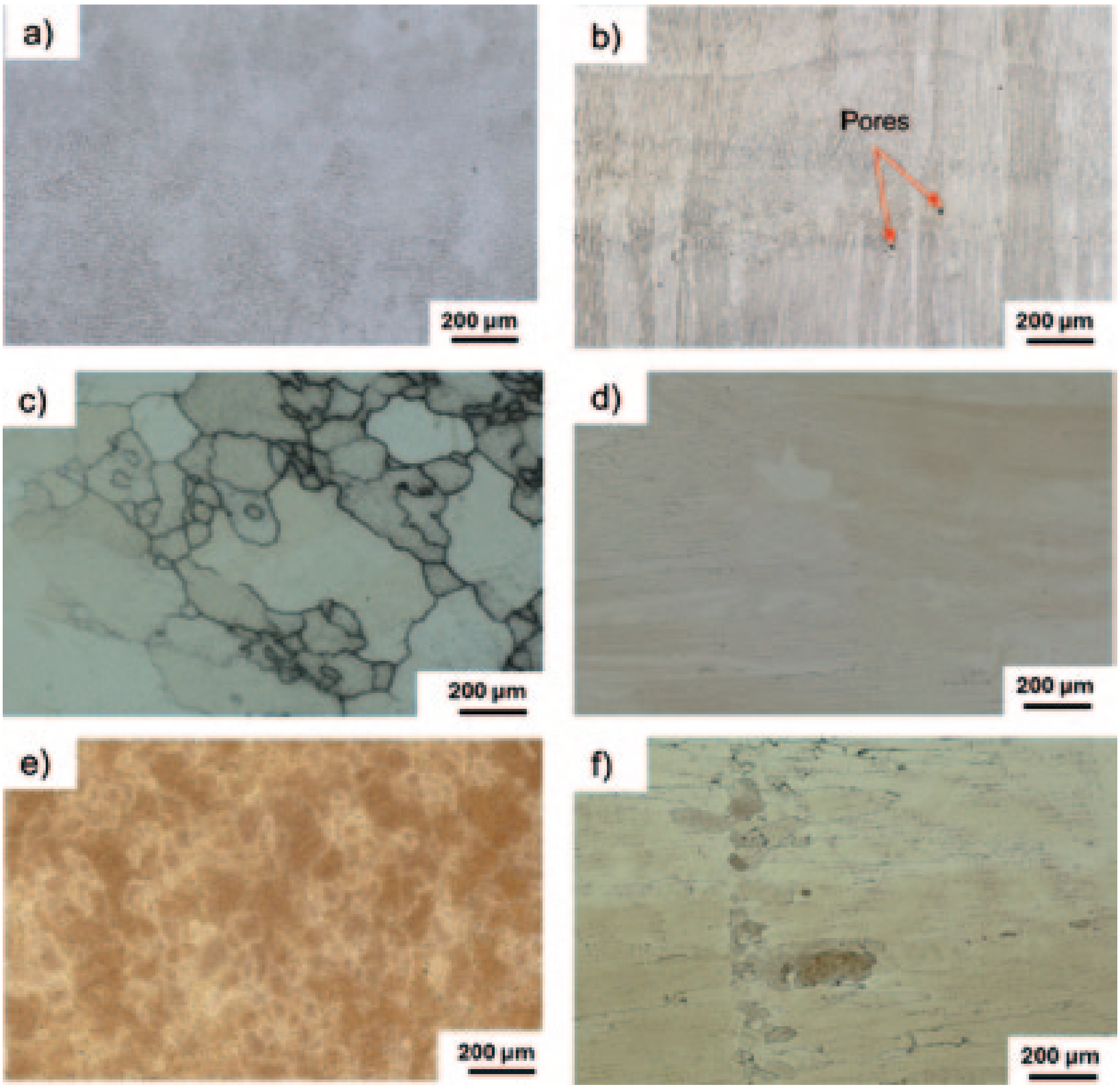

Fig. 6. Cross-section OM images of CMT 350 material variants in two perpendicular planes (a), c), e) – XY plane and b), d), f) – YZ plane): a), b) as deposited; c), d) after HIP process; e), f) after HIP and HT

porosity, mitigation of microsegregation, and dissolution of the detrimental Laves phase. Furthermore, HIP processing reduced the anisotropy of mechanical properties associated with the directional solidification and layer-by-layer deposition inherent to the WAAM process.

The highest mechanical performance was achieved after the combined hot isostatic pressing and heat treatment (HIP + HT). In this condition, the hardness increased to approximately 460–490 HV0.2, corresponding to nearly a twofold increase compared with the as-built WAAM-CMT condition and slightly exceeding that of the reference material. Simultaneously, the yield strength ($R_{2.0}$) and ultimate tensile strength (R_m) increased to approximately 870-1150 MPa and 1100-1250 MPa, respectively, depending on specimen orientation. These values approached, and in some cases exceeded, those of the reference material (Fig. 13-14). The observed strengthening is primarily associated with the precipitation of coherent γ' and γ'' phases during aging, accompanied by further microstructural homogenization.

4. Discussion

The results obtained indicate a strong dependence of the mechanical properties of Inconel 718 alloy manufactured by the WAAM-CMT process on the applied post-processing treatment. In the as-built condition, the alloy exhibits a cast-like micro-

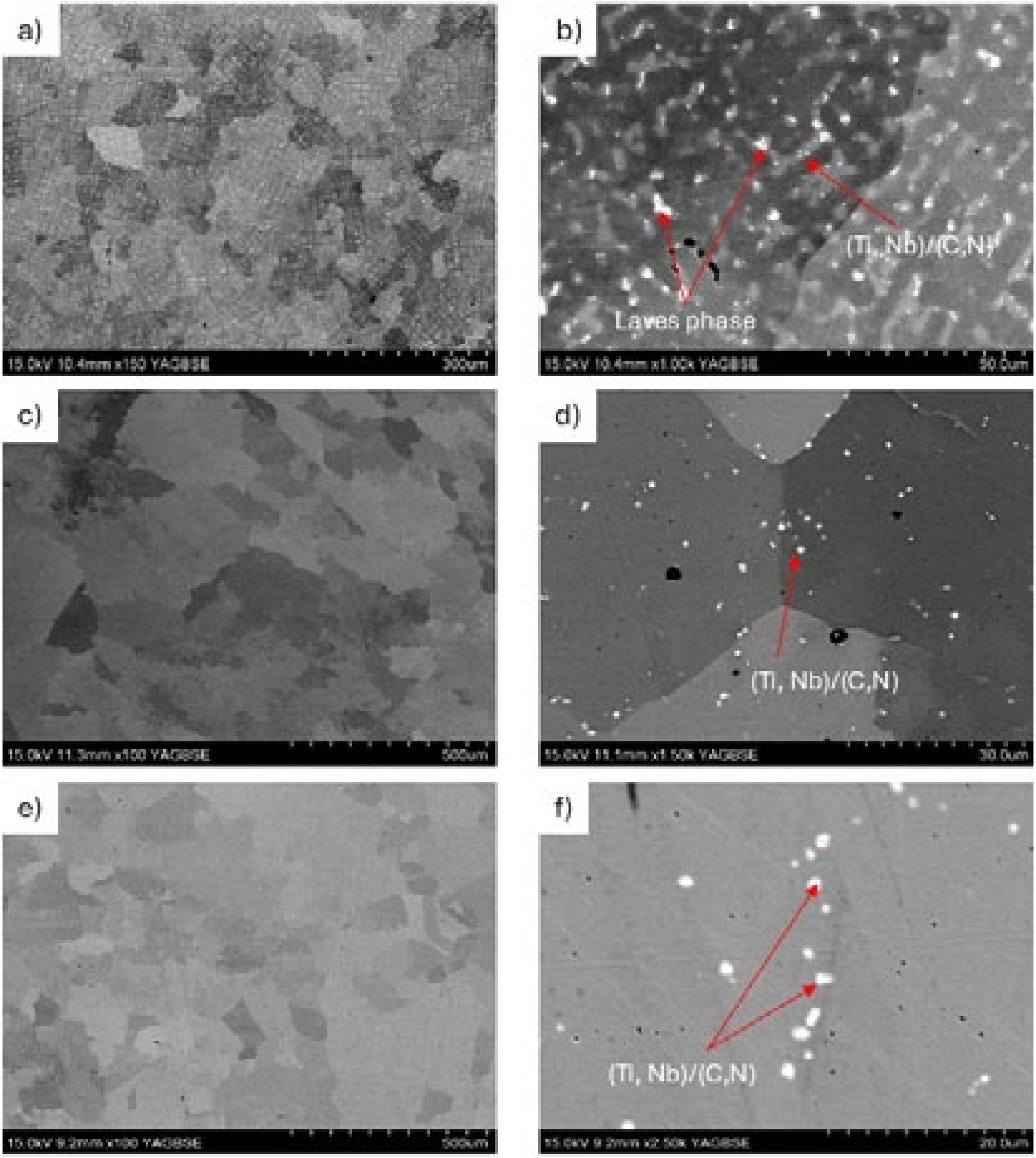

Fig. 7. SEM images of CMT150 in all variants (XY plane): a), b) as deposited; c), d) after HIP process; e), f) after HIP and HT

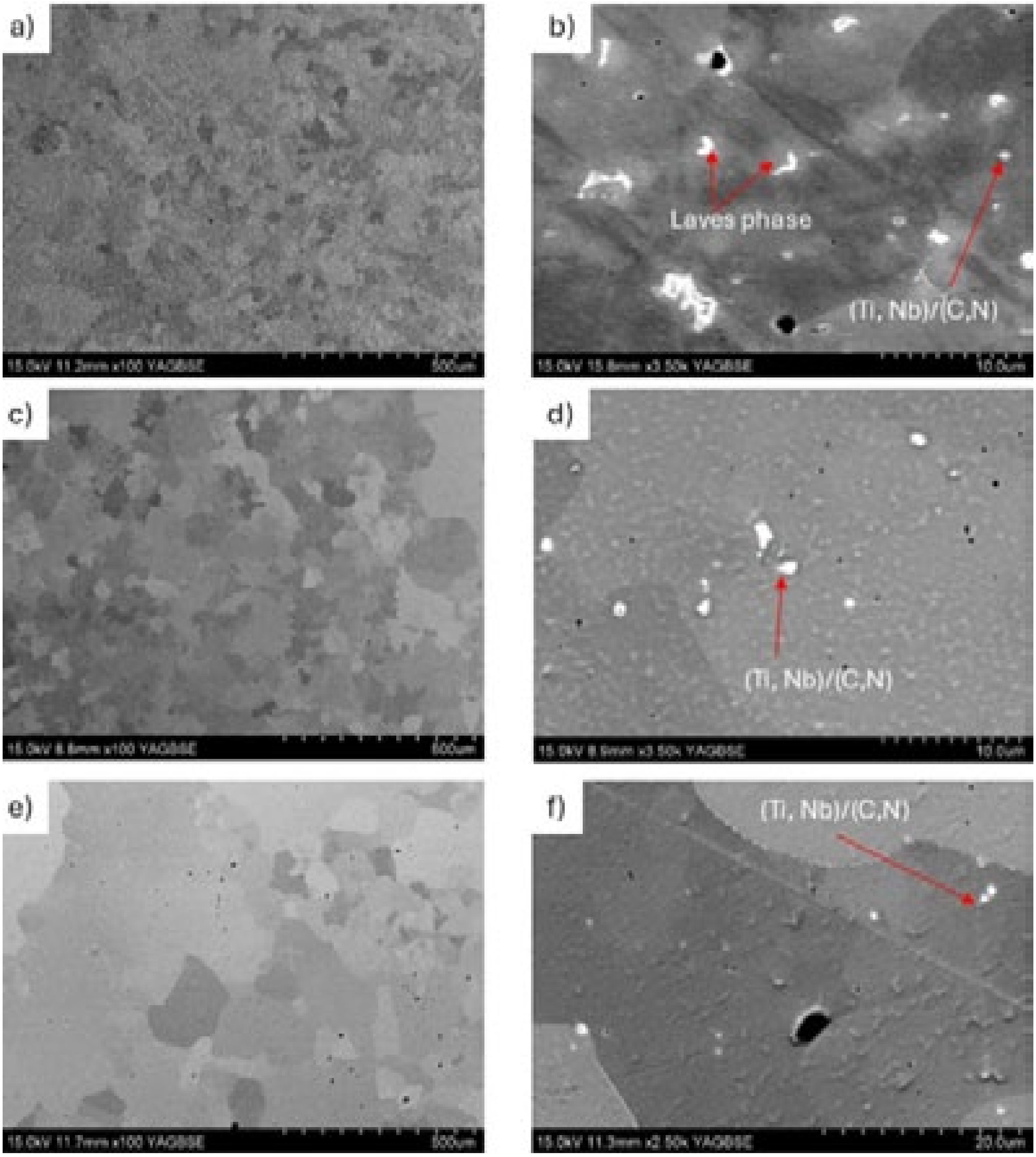

Fig. 8. SEM images of CMT150AC in all investigated states (XY plane): a), b) as deposited; c), d) after HIP process; e), f) after HIP and HT

structure characteristic of WAAM-produced IN718 materials, comprising columnar dendrites aligned with the build direction, interlayer banding, and pronounced microsegregation with the presence of interdendritic Laves phase, γ/Laves eutectic, and MC-type carbides (NbC) and nitride (TiN).

This microstructural state is consistent with descriptions reported in the literature [16-18] for WAAM IN718 materials, in which directional solidification and repeated thermal cycles lead to anisotropy as well as the formation of segregated interdendritic constituents, including Laves phase precipitates and γ/Laves eutectic. The relatively low hardness and tensile strength observed in the as-built condition are therefore expected.

The increase in hardness and strength after applying the HIP process is consistent with the well-known role of high-temperature hot isostatic pressing in closing porosity, reducing local stress concentrators, and partially homogenizing regions prone to interdendritic segregation. In the case of WAAM IN718, this effect is particularly significant, as the as-built material contains regions enriched in Laves phase, which adversely affects ductility and simultaneously creates local Nb-depleted zones.

The HIP cycle conducted at 1200°C under a pressure of 200 MPa was sufficiently intensive to disrupt and dissolve the primary network of the Laves phase and to reduce the material's sensitivity to defects, which explains the observed improvement in hardness, yield strength, and tensile strength. At the same time, the high temperature of the HIP process promotes recrystallization and grain growth, as well as partial elimination of the original dendritic morphology – Figs. 7c), d); 8c), d); 10a), b).

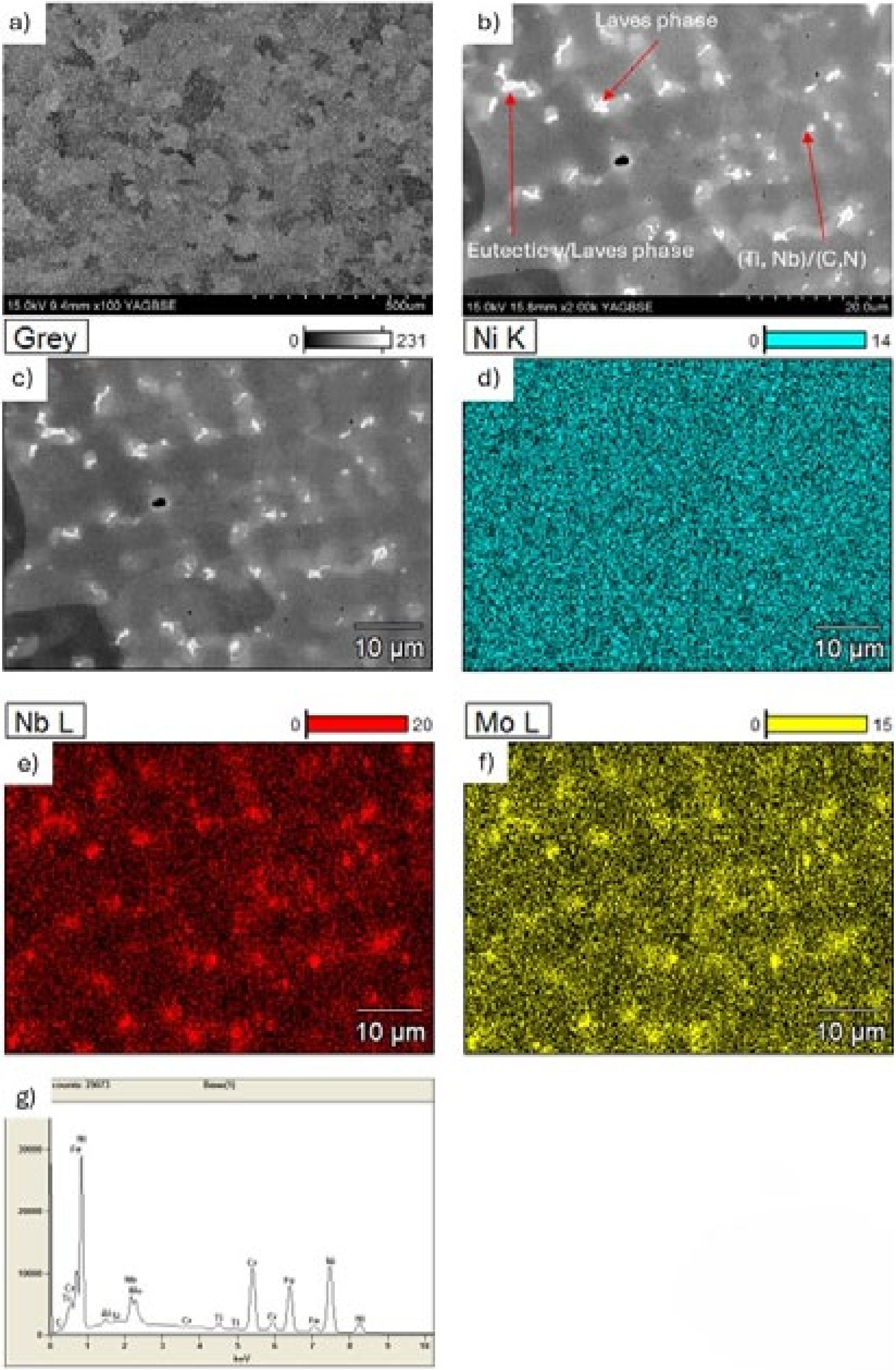

Fig. 9. SEM images of CMT350 in as deposited state: a), b) corresponding EDS results c)-g)

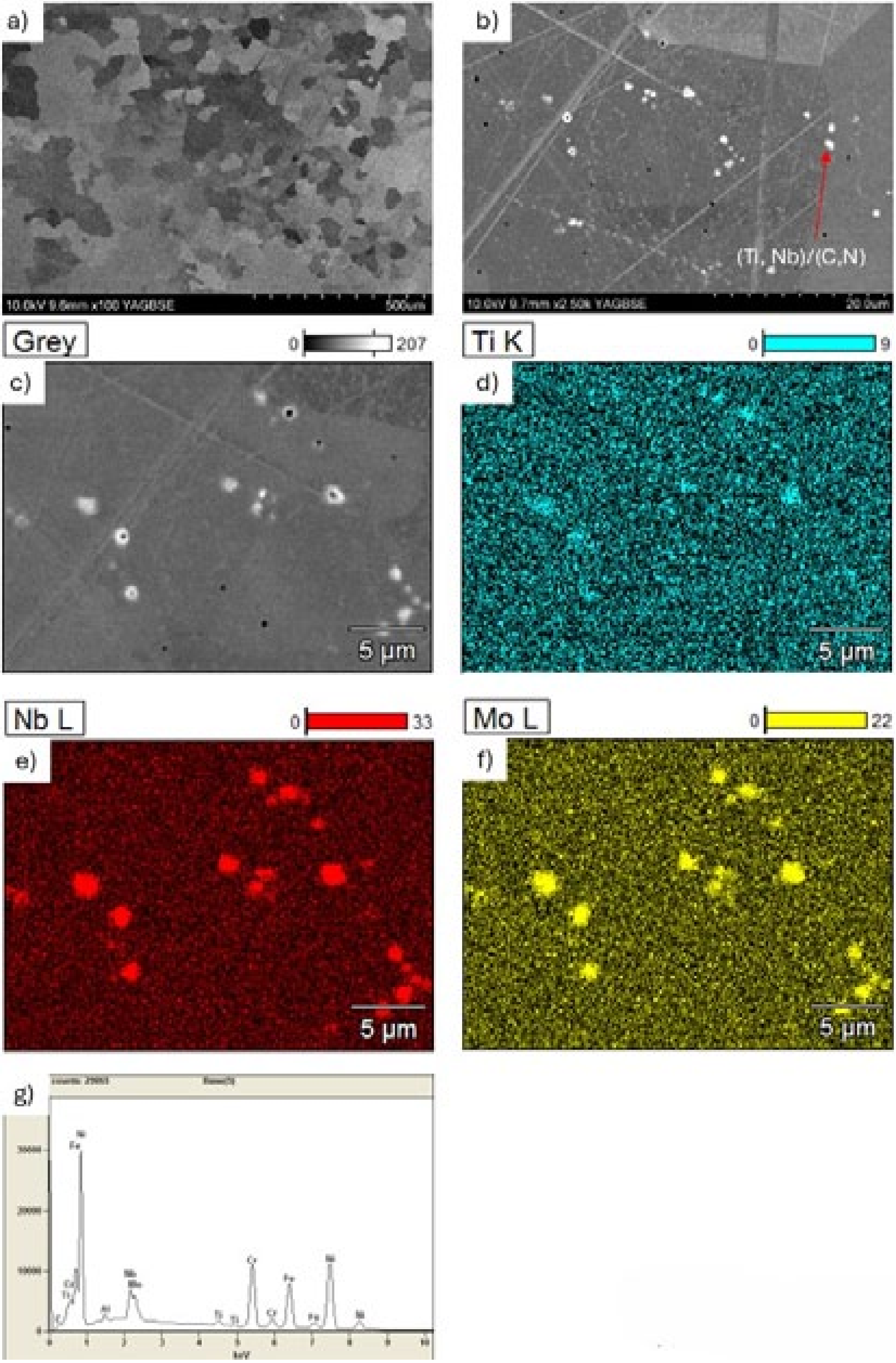

Fig. 10. SEM images of HIP treated CMT350: a), b) corresponding EDS results c)-g)

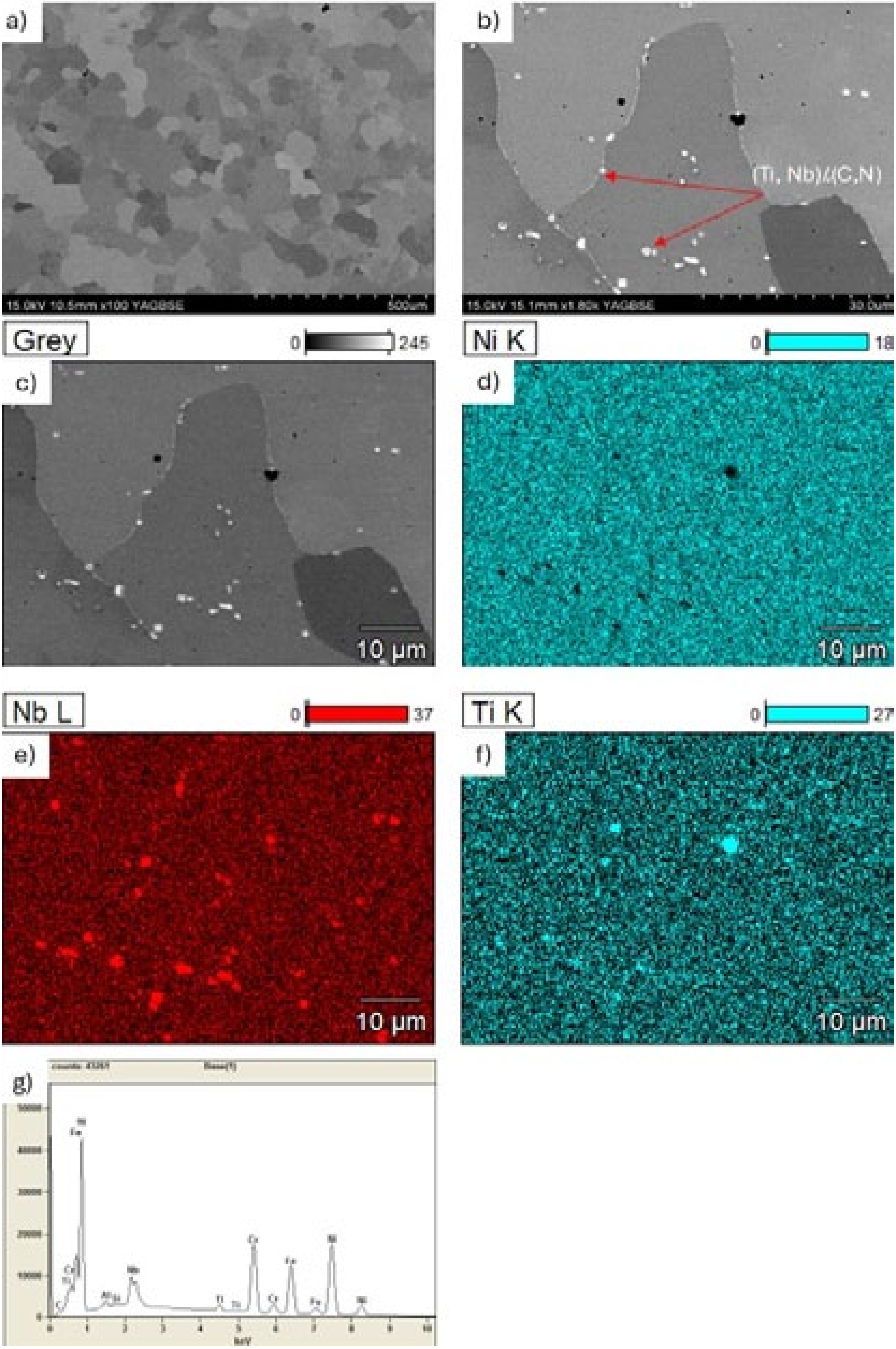

Fig. 11. SEM images of heat treated CMT350: a), b) corresponding EDS results c)-g)

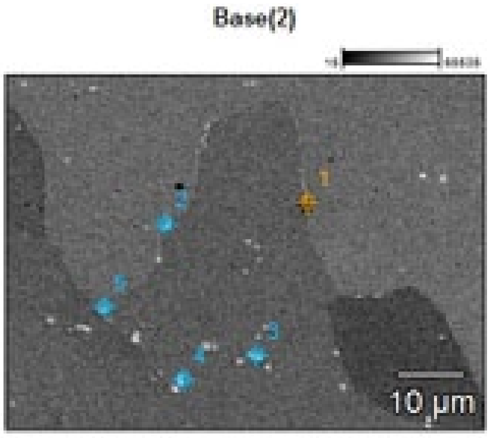

Elements, % by weight												
	C	N	Mg	Al	Si	Ti	V	Cr	Fe	Ni	Nb	Mo
Point 1	2.9	9.4	0.3			60.2		2.6	1.9	4.7	18.1	
Point 2	2.1			0.3		4.5	0.1	11.5	12.7	31.7	37.1	
Point 3	4.1					9.5		3.4	2.8	6.4	73.7	
Point 4	3.7					8.0		5.4	5.3	10.1	67.6	
Point 5	0.6			0.5	0.3	0.9		17.9	19.9	51.9	5.0	3.0

Fig. 12. Heat treated CMT350 material – results of EDS mapping quantitative analysis

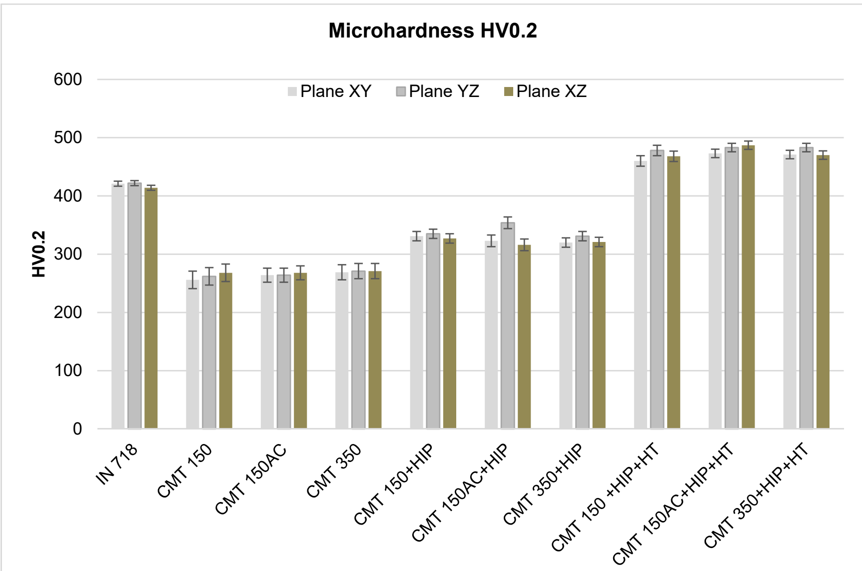

Fig. 13. Comparison of microhardness HV0.2 for all material variants

The greatest improvement in properties was achieved after applying a combined HIP and heat treatment process. Solution treatment performed at approximately 970°C for 1 hour followed by water quenching leads to the dissolution of the residual Laves phase and redistribution of Nb within the γ matrix, creating a more chemically homogeneous initial state for subsequent aging. This step is critical for IN718, as the amount of Nb retained in solid solution determines the precipitation potential of the strengthening γ'' phase [13,18].

Subsequently, a two-stage aging process was applied, consisting of holding at 720°C for 8 hours followed by furnace cooling to 620°C, and then a second aging step at 620°C for 8 hours with final air cooling. This treatment promotes the formation and stabilization of fine, coherent γ' and γ'' precipitates [13,17,18]. These precipitates constitute the primary source of the significant increase in hardness and strength observed after HIP + HT processing, with the resulting property levels approaching or even exceeding those of the reference material.

An additional effect of the applied post-processing treatment is the reduction of microstructural anisotropy. WAAM-CMT material in the as-built condition retains a strong texture associated with the deposition direction and a layered morphol-

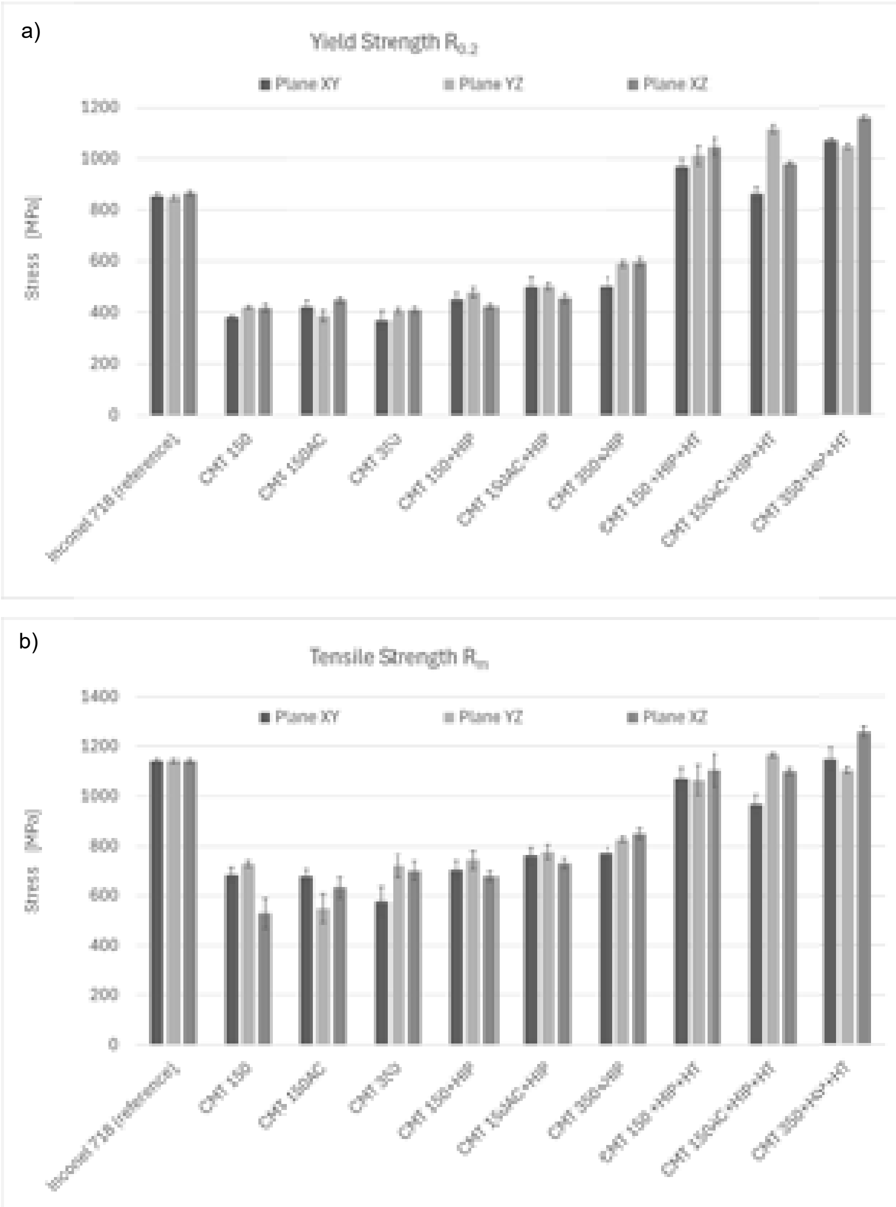

Fig. 14. Comparison of mechanical properties a) R_m and b) $R_{2.0}$) for all material variants

ogy, both of which contribute to the directional dependence of mechanical properties. The HIP process partially reduces this anisotropy by eliminating pores and decreasing chemical and phase segregation in interdendritic regions.

After solution treatment and aging, the material exhibits more homogeneous behavior regardless of orientation. This observation is consistent with the general conclusion that post-processing heat treatment is a key step not only for improving absolute strength properties but also for enhancing the uniformity of properties in WAAM-manufactured IN718 materials.

In summary, the results confirm that the mechanical properties of Inconel 718 alloy produced by WAAM-CMT are governed by sequential post-processing. The heterogeneity of the solidification microstructure in the as-built condition limits material performance; the HIP process leads to defect elimination, reduction of alloying element segregation, dissolution of the Laves phase, and recrystallization of the matrix, while heat treatment (solution treatment + aging) activates the full precipitation strengthening effect. Such a processing route is therefore necessary for WAAM IN718 to achieve properties comparable to those obtained by conventional manufacturing methods.

5. Conclusions

Based on the conducted research, the following conclusions can be drawn:

- IN718 alloy manufactured using the WAAM-CMT method in the as-built condition exhibits significantly reduced mechanical properties compared to material produced by conventional methods (with strength parameters nearly two times lower).
- Appropriately selected post-processing treatments following WAAM-CMT (densification via hot isostatic pressing,

HIP, followed by precipitation hardening) effectively restore the mechanical properties to a level comparable with the reference material. This effect is associated with sequential post-processing. Hot isostatic pressing after printing leads to the elimination of defects, reduction of alloying element segregation, recrystallization of the matrix, and the dissolution of the Laves phase and γ/Laves eutectic. In turn, heat treatment (solution treatment + aging) additionally activates the full precipitation strengthening effect.

- A significant improvement in mechanical properties was achieved after applying combined HIP and heat treatment (HIP + HT), resulting from a complete reconstruction of the material's microstructure relative to the as-built WAAM-CMT condition. After post-processing, hardness increased nearly twofold compared to the as-built state, while the values of yield strength ($R_{2.0}$) and ultimate tensile strength (R_m) reached approximately 870-1150 MPa and 1100-1250 MPa, respectively, approaching – and in some cases even exceeding – the properties of the reference material.

Acknowledgments

The research was carried out at the Faculty of Materials Science and Engineering of Warsaw University of Technology as part of the 2026 subsidy for the project "Shaping the structure and functional properties of metallic materials manufactured by additive manufacturing".

REFERENCES

[1] L.L. Parimi, G. Ravi, D. Clark, M.M. Attallah, Microstructural and texture development in direct laser fabricated IN718. Mater. Charact. **89**, 102-111 (2014).
DOI: https://doi.org/10.1016/j.matchar.2013.12.012

[2] M. Shahwaz, P. Nath, I. Sen, A critical review on the microstructure and mechanical properties correlation of additively manufactured nickel-based superalloys. J. Alloys Compd. **907**, 164530 (2022).
DOI: https://doi.org/10.1016/j.jallcom.2022.164530

[3] G.M. Volpato, U. Tetzlaff, M.C. Fredel, A comprehensive literature review on laser powder bed fusion of Inconel superalloys. Addit. Manuf. **55** (2022).
DOI: https://doi.org/10.1016/j.addma.2022.102871

[4] K. Majchrowicz, Z. Pakieła, J. Kamiński, et al., The Effect of Rhenium Addition on Microstructure and Corrosion Resistance of Inconel 718 Processed by Selective Laser Melting. Metall. Mater. Trans. A Phys. Metall. Mater. Sci. **49**, 6479-6489 (2018).
DOI: https://doi.org/10.1007/s11661-018-4926-3

[5] H. Pan, T. Dahmen, M. Bayat, et al., Independent effects of laser power and scanning speed on IN718's precipitation and mechanical properties produced by LBPF plus heat treatment. Mater. Sci. Eng. A **849**, 143530 (2022).
DOI: https://doi.org/10.1016/j.msea.2022.143530

[6] M. Amirjan, H. Sakiani, Effect of scanning strategy and speed on the microstructure and mechanical properties of selective laser melted IN718 nickel-based superalloy. Int. J. Adv. Manuf. Technol. **103**, 1769-1780 (2019).
DOI: https://doi.org/10.1007/s00170-019-03545-0

[7] J. Koto (2nd Ed.), Application of Subsea Tree Deep Water, Ocean & Aerospace Research Institute, Indonesia (2017).

[8] Y. Guan, J. Luo, M. Duan, S. Huang, Risk analysis of subsea x-mas tree leakage. Advances in Structural Engineering and Mechanics (2015). https://www.i-asem.org/publication_conf/asem15/7.ICOSE15/1w/W3H.3.MS622_2124F1.pdf, accessed: 24.03.2014

[9] K. Adamowicz, P. Sarna, W. Szatko, Safety In Subsea Petroleum Production Systems: Subsea Christmas Tree Case Study. Technical Transactions Mechanics 2-M (2016).

[10] N. Xi, X. Fang, Y. Duan, et al., Wire arc additive manufacturing of Inconel 718: Constitutive modelling and its microstructure basis. J. Manuf. Process. **75**, 1134-1143 (2022).
DOI: https://doi.org/10.1016/j.jmapro.2022.01.067

[11] B. Wu, Z. Pan, D. Ding, et al, A review of the wire arc additive manufacturing of metals: properties, defects and quality improvement. J. Manuf. Process. **35**, 127-139 (2018).
DOI: https://doi.org/10.1016/j.jmapro.2018.08.001

[12] P. Kumar, R.K. Raj Singh, S.K. Sharma, Effect of process parameters on wire-arc direct energy deposited Inconel 718 superalloy. Rapid Prototyp. J. **31**, 950-967 (2025).
DOI: https://doi.org/10.1108/rpj-05-2023-0176

[13] C.E. Seow, H.E. Coules, G. Wu, Wire + Arc Additively Manufactured Inconel 718: Effect of post-deposition heat treatments on microstructure and tensile properties. Mater. Des. **183**, 108157 (2019).
DOI: https://doi.org/10.1016/j.matdes.2019.108157

[14] P. Li, J. Andersson, M. Igestrand, et al., Feasibility study of WAAM application on superalloy Inconel 718 in aerospace industry – impact of shielding gas. Weld. Int. p. 1-13 (2025).
DOI: https://doi.org/10.1080/09507116.2025.2563764

[15] G. Liu, Y. Su, S. Xin, et al., Enhanced wear resistance of Ti reinforced Inconel 718 superalloy manufactured by laser directed energy deposition. Mater. Charact. **20**, 113736 (2024).
DOI: https://doi.org/10.1016/j.matchar.2024.113736

[16] K. Hartl, C. Wallis, M. Bielik, P. Curti, M. Stockinger, Characterization of the Anisotropic Behaviour of Inconel 718 Parts Manufactured by Wire Arc Additive Manufacturing. In Proceedings of the 10th International Symposium on Superalloy 718 and Derivatives. Springer International Publishing, The Minerals, Metals & Materials Series 789-805 (2023).
DOI: https://doi.org/10.1007/978-3-031-27447-3_47

[17] N. Haldar, S. Anand, S. Datta, et al., On Fabrication of Inconel 718 Slab by Wire Arc Additive Manufacturing: Study of Built Microstructure and Mechanical Properties. Arab. J. Sci. Eng. **49**, 2045-2063 (2024).
DOI: https://doi.org/10.1007/s13369-023-08095-y18

[18] F. W. Cipriano Farias, V. Rebelo Duarte, J. da Cruz Payão Filho, N. Schell, E. Maawad, M. Bordas-Czaplicki, J.P. Oliveira, Arc-based directed energy deposited Inconel 718: role of heat treatments on high-temperature tensile behavior. Materials Research Letters **12** (2), 97-107 (2024).
DOI: https://doi.org/10.1080/21663831.2023.2297734